

## ENC-2022-0468

# DETECTION OF CALCIUM CARBONATE PRECIPITATION BY SENSORS BASED ON FIBER OPTIC BRAGG NETWORKS

**Luila Abib Saidler**

**Bruno Venturini Loureiro**

**Arnaldo Gomes Leal Junior**

**Leandro Cassa Macedo**

**Luka Simas Maximiano**

UFES – Universidade Federal do Espírito Santo

Departamento de Engenharia Mecânica – CTIII

Av. Fernando Ferrari, Campus Universitário Goiabeiras, Vitória – ES, 29060-973

luila.saidler@edu.ufes.br

**Renato do Nascimento Siqueira**

IFES – Instituto Federal do Espírito Santo

Rodovia BR 101 Norte Km 58, Litorâneo, São Mateus - ES, 29932-540

renatons@ifes.edu.br

**Abstract.** Scale has been recognized as a major operational problem in oil production. This mineral deposition comes from the accumulation of inorganic salts and interferes with the guarantee of flow, causing production losses and equipment changes. In particular, the precipitation of calcium carbonate ( $\text{CaCO}_3$ ) can occur from the incompatibility between the chemical compositions of the formation and injection waters and/or by the thermodynamic changes of the system during production. In this scenario, estimating the mass of precipitated crystals as a function of operational variables is necessary to propose actions to mitigate scale in producing wells. The fiber optic sensor technology based on Fiber Bragg Gratings (FBG) has been used in several important application areas from the measurement of spectral variations. These sensors have intrinsic sensitivity to variations of temperature and deformation, thus, they are important devices for the sensing of several physical quantities. The aim of this article, therefore, is to present the response of fiber optic systems to the measurement of deposited mass of  $\text{CaCO}_3$  crystals. The experimental setup for this study consists of a reservoir for mixing aqueous solutions of  $\text{NaHCO}_3$  and  $\text{CaCl}_2$ , under controlled temperature conditions, a precision balance to measure the mass of crystals formed, an optical interrogator, a computer and a part developed in 3D printer to receive the inlay coupons with the FBG sensors. The results are used to establish a correlation between the optical fiber sensor response and the precipitated  $\text{CaCO}_3$  mass, in order to develop a method of measuring mass accumulation rates through optical fiber sensor systems.

**Keywords:** Calcium carbonate scaling, oil production, fiber bragg gratings sensors.

## 1. INTRODUCTION

Oil continues to play an important role in the energy matrix of Brazil and the world. Intrinsic problems to its production lead to production losses, equipment changes, execution of maintenance services leading to an increase in production costs. In the oil industry, inorganic fouling is one of the main operational problem and the losses associated with it reach, on a global scale, the order of 1.4 billion dollars per year (FRENIER; ZIAUDDIN, 2008).

The fouling can cause operational problems related to the flow guarantee due to the partial obstruction of the flow section which causes an additional pressure drop is generated and consequently can restrict the oil production.

In general, predictive tools for fouling are based only on thermodynamic models, which provide a scaling potential based on water composition, pressure, and temperature, and do not provide information on the time required to completely block flow or the amount of fouling, encrusted material. In addition to the thermodynamic and kinetic aspects of the problem, the flow dynamics can also exert a significant influence on the fouling rate and on the fouling mechanisms of crystal growth, agglomeration, deposition and surface adhesion (MARTINS et al., 2020).

It is known that the fiber optic sensor technology based on Fiber Bragg Gratings (FBG) has been used in several important application areas from the measurement of spectral variations. These sensors have intrinsic sensitivity to variations in temperature and deformation, thus, they are important devices for the sensing of several physical quantities.

Calcium carbonate,  $\text{CaCO}_3$ , is one of the most common scale components found in oilfield production wells and surface facilities (ZHANG et al, 2001). As the costs to remove a scale are high (CRABTREE et al., 1999), understanding the beginning of crystal formation is important. In this sense, the objective of this article is to present the response of a fiber optic instrumentation system to the measurement of deposited mass of crystals, specifically of  $\text{CaCO}_3$ .

## 2. THE CARBONATE SCALE PROBLEM IN THE OIL PRODUCTION

Due to the discovery of large carbonate reservoirs in the pre-salt, the issue of fouling gains importance in terms of guaranteeing flow for the production of oil. Scale is an accumulation of different materials that can lead to the obstruction of a pipeline and prevent the flow of fluids from the beginning of production to the abandonment of a well which can affect production lines, valves, casings and subsea equipment (CRABTREE et al. al, 1999).

The depositions by insoluble salts (mineral scale) most commonly found in oil production environments are: calcium sulfate ( $\text{CaSO}_4$ ), calcium carbonate ( $\text{CaCO}_3$ ), barium sulfate ( $\text{BaSO}_4$ ), strontium sulfate ( $\text{SrSO}_4$ ), iron (II) ( $\text{FeCO}_3$ ) and iron (II) hydroxide ( $\text{Fe}(\text{OH})_2$ ), with calcium carbonate deposition and incrustation being the main focus of this work.

Calcium carbonate ( $\text{CaCO}_3$ ) is an inorganic salt that forms when an aqueous environment is saturated with carbonate anions ( $\text{CO}_3^{2-}$ ) and calcium cations ( $\text{Ca}^{2+}$ ), according to Equation 1.



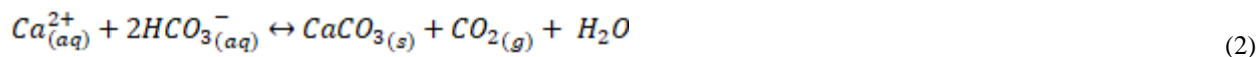
Scale is induced because before drilling and production begins, the species dissolved in the fluids are in equilibrium with the reservoir environment. Precipitation reactions begin to occur when external forces act on the fluids, that is, when there is a disturbance that favors the imbalance reached after thousands of years of thermal, chemical and mechanical interaction between rock and fluids (CRABTREE et al. al, 1999).

These external forces are mainly due to runoff and its consequences and to the mixing of fluids – mainly the mixing of reservoir water with other waters, such as injection water – incompatible in terms of chemical species (MUHAMMAD et al, 2018).

For the onset of precipitation and consequent formation of crystals, the occurrence of three simultaneous factors is necessary (YORK; SCHORLE, 1997): supersaturation, nucleation and contact time.

Initially small solid particles are formed, which tend to cluster in an orderly manner which gives rise to a mineral. Depending on the ordering of these particles, calcium carbonate minerals receive different names, such as calcite, aragonite, vaterite, among others, with calcite being the most commonly found mineral (AL NASSER et al., 2008) because it is more stable (COWAN; WEINTRITT, 1976). The process of forming the first solid particles from ions is called nucleation. After nucleation, crystal growth is provided by the grouping of new particles.

Davies and Scott (2006) reported the sequence for the formation of this salt, represented by the global reaction of equation 2, in which carbon dioxide ( $\text{CO}_2$ ) first dissolves in water ( $\text{H}_2\text{O}$ ) to form carbonic acid ( $\text{H}_2\text{CO}_3$ ); then carbonic acid ( $\text{H}_2\text{CO}_3$ ) dissociates into carbonate ( $\text{CO}_3^{2-}$ ) and bicarbonate ( $\text{HCO}_3^-$ ), which lowers the pH; finally, carbonate ions ( $\text{CO}_3^{2-}$ ) interact with calcium ( $\text{Ca}^{2+}$ ) to precipitate calcium carbonate ( $\text{CaCO}_3$ ).



Several factors contribute to the deposition of calcium carbonate particles, such as temperature, pressure, chemical balance, pH, residence time and ionic strength (Yap et al, 2010), because these variables influence its solubility.

$\text{CO}_2$  is possibly the chemical species that most affects the precipitation of calcium carbonate. This is due to the fact that  $\text{CO}_2$  tends to remain dissolved in water at high pressures, and with flow and depressurization, carbon dioxide readily leaves the liquid phase and passes to the gaseous phase (MOGHADASI et al., 2003). which is known as a  $\text{CO}_2$  flash.

A combination of factors influences the solubility of carbon dioxide in the reservoir water. Lower temperature near the surface increases solubility, but lower pressures cause loss of carbon dioxide to compensate for the gain from temperature influence. In almost all cases, the loss of carbon dioxide by pressure drop is the biggest effect and, therefore, there is the appearance of calcite deposits (DAVIES; SCOTT, 2006).

Moghadas et al. (2006) studied the effects of temperature on the formation of different types of scale and found that  $\text{CaCO}_3$  scale increases with increasing temperature. Regarding the pressure, the increase in  $\text{CaCO}_3$  precipitated with the decrease in pressure is due both to the direct reduction of the mineral solubility, and to the flash of  $\text{CO}_2$  from

the solution. As a result of the exit of carbon dioxide from the aqueous medium, there is an increase in pH in the solution, which makes CaCO<sub>3</sub> even more insoluble. Thus, the possibility of the occurrence of CaCO<sub>3</sub> incrustations is evidenced by the increase in temperature and pH and decrease in pressure (HAMID et al., 2016; RAMSTAD et al., 2005).

The saturation index (SI) was proposed by Stiff and Davis (1952) to predict the scaling trend of mixed brine at different temperatures. SI is a scale prediction method widely used in oilfield production (ZHANG et al., 2001) and is given by Equation 3.

$$SI = \log (SR) \quad (3)$$

Where SR (saturation ratio) is the saturation ratio. For calcium carbonate it is described according to the Equation, with {Ca<sup>2+</sup>}, {CO<sub>3</sub><sup>2-</sup>} being the activities of the species measured in the saline solution and K<sub>sp</sub> the solubility product (equilibrium constant) calculated for the thermodynamic conditions considered, according to Equation 4.

$$SR = \frac{\{Ca^{2+}\}\{CO_3^{2-}\}}{K_{sp}} \quad (4)$$

In view of the analysis of the SR values, the following can be obtained from the analysis of the SI values:

- If SI < 0 - dissolution potential of preexisting deposits;
- If SI = 0 - no dissolution potential and no deposition potential;
- If SI > 0 - solid deposit precipitation potential

Due to the complexity of predicting and quantifying fouling in the oil production process, the study of new technologies that allow this understanding of the kinetics of CaCO<sub>3</sub> formation is urgent. Therefore, the contribution of this article is to understand a proof of concept in which it aims to measure the mass deposition using sensors based on Bragg gratings, which from the wavelength reading, it is possible to predict the deposited mass of calcium carbonate. Through the proposed solution, it is possible to carry out interventions in the initial stage of fouling aiming at mitigating larger problems.

### 3. FIBER OPTIC IMPLEMENTATION IN CALCIUM CARBONATE MASS DETECTION

The use of optical fiber as a sensor occurs through the application of polymer fibers as Fiber Bragg Gratings (FBGs). FBGs are a permanent and periodic or quasi-periodic modulation of the refractive index of the fiber core along the propagation axis. This modulation is usually done over a few millimeters or centimeters (BROADWAY et al., 2019).

Fiber photosensitivity was observed for the first time through an experimental setup, which consists of a continuous blue light of wavelength  $\lambda = 488$  nm from an argon ion laser, launched on a small piece of nominal single-mode optical fiber, being its intensity of light reflected back from the monitored fiber (HILL; MELTZ, 1997).

Initially, as described by Hill and Meltz (1997), the intensity of reflected light is low, but after a period of a few minutes, it increases in intensity until almost all the light thrown on the fiber is reflected. The growth of reflected light was explained in a new non-linear effect called photosensitivity, changing the refractive index of the fiber. The change in refractive index is permanent in the sense that it will last for decades. Initially, photosensitivity was thought to be a phenomenon associated only with germanium-doped optical fibers. It was later observed in a wide variety of different fibers, many of which did not contain germanium as a dopant.

Historically, Bragg grids were first fabricated using internal writing and through holographic technique. Both these methods have been largely replaced by the phase mask technique which has the advantage of greatly simplifying the manufacturing process of FBGs but producing high-performance grids.

Another approach to grating fabrication is the dot-by-dot technique. In this method each perturbation of the grid index is written point by point. For grids with many index perturbations, the method is inefficient (HILL; MELTZ, 1997).

FBG-based fiber optic sensor technology has been used in several important application areas, from structural monitoring to chemical sensing. Practical and cost-effective systems are not far into the future, judging by recent advances in sensor-reading grids and instrumentation.

A very important advantage of an FBG sensor is that it is wavelength encoded. The shifts in the spectrum, seen as a narrowband reflection or dip in transmission, are independent of optical intensity and uniquely associated with each grid, as long as there is no overlap in each sensor stop-band.

Bock and Domanski (1989) evaluated the effect of high hydrostatic pressure of up to 200 MPa on polarization properties in highly birefringent fibers. It was found that an oscillatory behavior of the output signal leaving the fiber

and monitored in the plane parallel to one of its two main axes can be interpreted as being caused by an induced pressure increase of the wavelength duration parameter.

This effect can be applied to detect high hydrostatic pressure using properly configured fiber. With sufficiently high critical pressure, the wavelength increase can be strong enough to cause birefringence to disappear, as seen at 6 MPa pressure. This critical pressure, if determined experimentally, can be used effectively to determine the wavelength at atmospheric pressure. This means a new and simple method of measuring wavelength (BOCK; DOMANSKI, 1989).

An FBG sensor can also be used to measure electric and magnetic fields with special magnetostrictive and piezoelectric coatings on the fiber. These jackets produce deformations within the core that cause the Bragg wavelength to shift with the measured magnitude. The induced deformations are small and a reading technique that has fine resolution is usually required (HILL; MELTZ, 1997).

Any deformation, temperature change or polarization that varies the modal index or the pitch of the grid will change the wavelength, therefore the grid is an intrinsic sensor that changes the spectrum of an incident signal by coupling the energy to other modes of fiber. In the simplest case, the incident wave is coupled in a mode similar to the counter-propagation and thus reflected (HILL; MELTZ, 1997).

In the work developed by Golnabi (2002), the design and operation of an opto-mechanical sensor for mass measurements are reported. This device uses a pair of optical fibers and a reflective coated lens. The modulation of light intensity is based on the relative motion of the lens due to a certain mass in relation to the optical fibers. The modulated intensity because of the weighing mass was measured using a digital voltmeter. A full range sensitivity of about 11.5 mV/g for a dynamic range of 80 g is achieved. A mass resolution greater than 0.25 g was measured with this device. The measured output response is verified against the theoretical expected and general agreement observed. A comparison with similar experimental results shows advantages of this method and potential use of such a sensor for mass-average measurements.

Thus, the precipitation of calcium carbonate can be identified by changing the wavelength, but with its due compensation for temperature, pressure and other phenomena (LEAL-JUNIOR et al., 2018).

#### 4. EXPERIMENTAL METHODS AND PROCEDURES

To evaluate the ability of the FBG to measure the deposited mass of calcium carbonate, an experimental bench was set up consisting of an acrylic reservoir (a) to receive the aqueous solutions, a precision balance (b) to measure the mass of crystals formed in the upper part of a metallic plate deposited at the bottom of the reservoir, an optical interrogator Micron Optics SM125 (c) and a computer to acquire the information. The assembly can be seen in Figure 1.

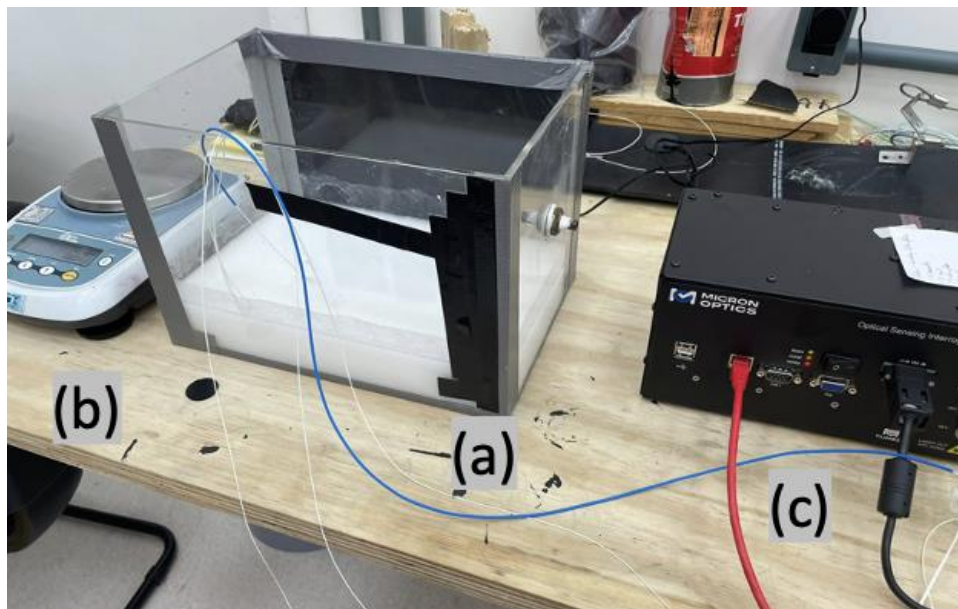


Figure 1. Experimental bench for calcium carbonate deposited mass tests.

The fiber optic sensors were mounted on rectangular metal sheets and three tests were performed to evaluate the response of the sensors in relation to mass deposition, namely:

- A. Characterization of the sensor response as a function of temperature
- B. Sensor response to controlled mass deposition
- C. Tests in the reservoir with the solutions and crystal formation

Test A consists of evaluating the Bragg wavelength in relation to temperature. The characterization was carried out in an oven with an initial temperature of 24°C to a final temperature of 45°C, with steps of 5°C. The length of the Bragg wave was measured using the optical interrogator.

Test B consists of making the mass position over the sensitive region of the optical fibers to evaluate the length of the Bragg wavelength in relation to the mass position. Up to 50 grams were used, measured with the aid of a scale. The Bragg wavelength was also measured using the optical interrogator.

Tests A and B are important to generate the characteristic curves of the sensors since both are sensitive to both temperature and mass deposition (strain). Therefore, they are performed in isolation, that is, in test A, only temperature variation is evaluated and in test B, mass deposition is evaluated at constant temperature. Therefore, tests A and B precede test C.

For test C, one liter of saturated solution of Sodium Bicarbonate ( $\text{NaHCO}_3$ ) and one liter of saturated solution of Calcium Chloride ( $\text{CaCl}_2$ ) were previously prepared and these solutions were left to rest. The methodology for analyzing the deposited mass involved weighing the sensor element before and after the test, after mixing the solutions in the acrylic reservoir, as shown in Figure 2. However, the sensitive area does not occupy the entire area of the plate, so it was considered a uniform mass distribution on the plate, evaluated by micrometer measuring the thickness in different positions of the plates and by the surface image generated by the Sensofar S Neox 090 profilometer. Subsequently, the deposition on the sensors was estimated from the difference in areas.

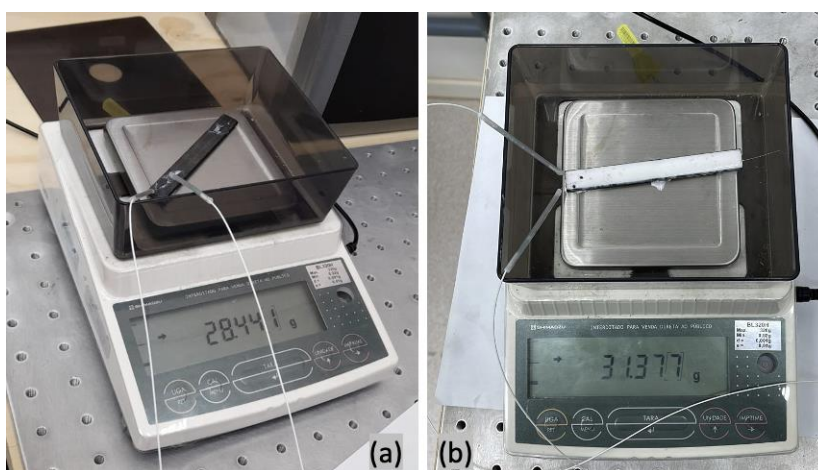


Figure 2. Methodology of analysis of the deposited mass: (a) weight before the beginning of the test and (b) weight after the end of the test.

## 5. RESULTS

One of the considerations made in this work is in relation to the analysis of mass deposition uniformity, as this directly affects the design of the sensors (quantity and position of the sensors). Four plates (all without fiber) were analyzed for the cases with and without deposited mass. In the results obtained by measuring the thickness by micrometer observed in Figure 3, there are only small variations in uniformity, in which the curves can be considered practically parallel.

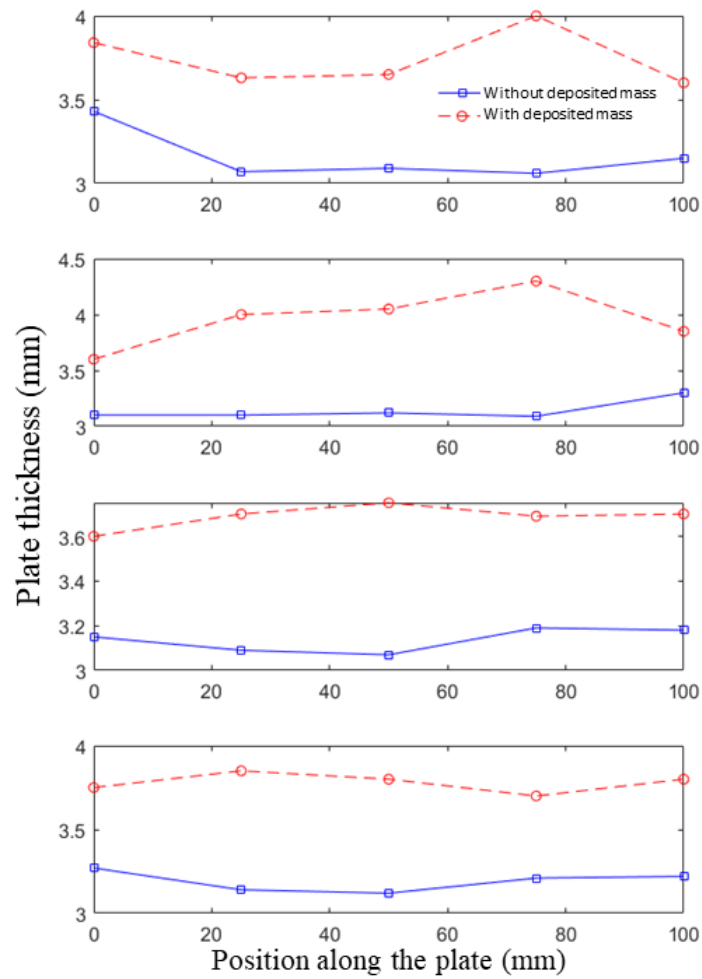


Figure 3. Analysis of mass deposition uniformity on the plates.

In Figure 4, there is an image of the surface obtained via profilometry, which corroborates the conclusion of the uniformity of the mass deposited on the plate. The height variation of the deposited crystals occurred in a range of approximately  $38.9 \mu\text{m}$  in an area of  $844.56 \times 706.56 \mu\text{m}$ .

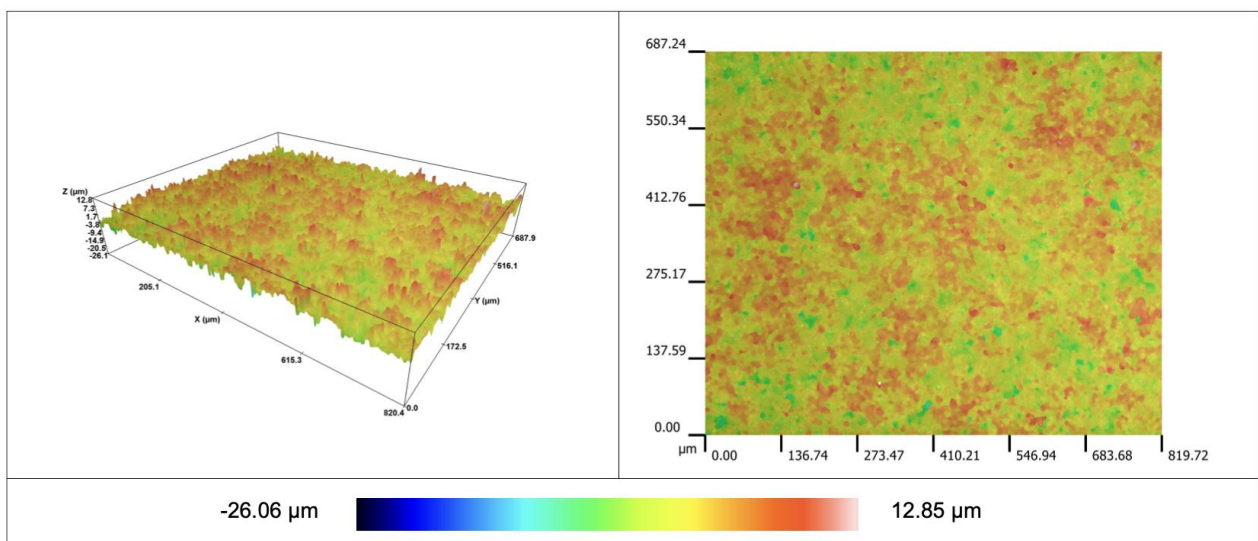


Figure 4. Image of the plate surface with calcium carbonate crystals for analysis of deposited mass uniformity.

The results obtained for test A, influence of temperature on the response of the sensors, are shown in Figure 5 and Figure 6. A linear response in relation to temperature can be seen, which can be used to compensate for the response of the measurement signal of deposited mass.

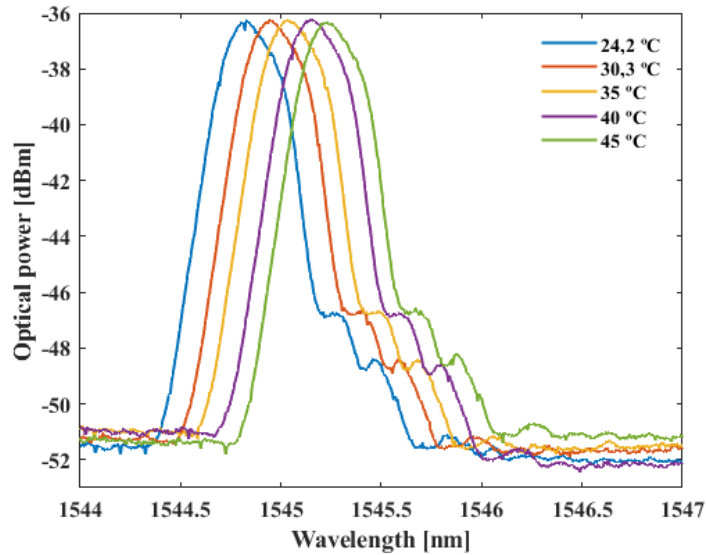


Figure 5. Variation of the reflected spectrum as a function of temperature.

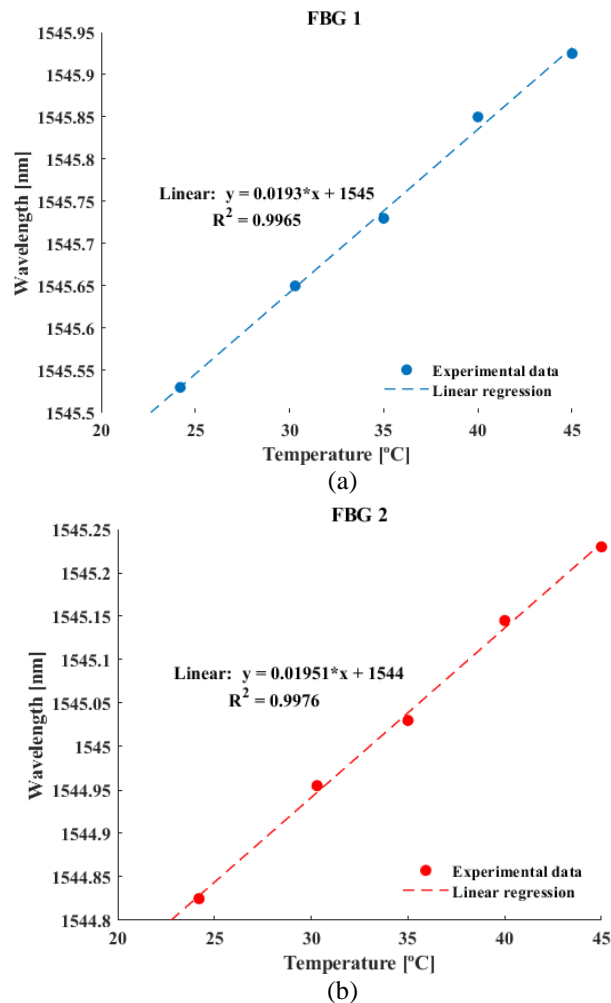


Figure 6. Temperature characterization for (a) FBG 1 and (b) FBG 2.

According to Figure 6, the reflected Bragg wavelength varied linearly with temperature. For FBG 1, the data were approximated by linear regression ( $R^2 = 0.9965$ ) with a sensitivity of  $0.0193 \text{ nm}/^\circ\text{C}$ . Similarly, the linear regression for FBG 2 ( $R^2 = 0.9976$ ) had a sensitivity of  $0.01951 \text{ nm}/^\circ\text{C}$ .

The results obtained for test B, influence of the deposited mass on the response of the sensors, are shown in Figure 7. As the sensors presented linear responses in all cases, a system of equations can be proposed to isolate the deposition responses of mass and temperature. Therefore, the need for two sensors arises.

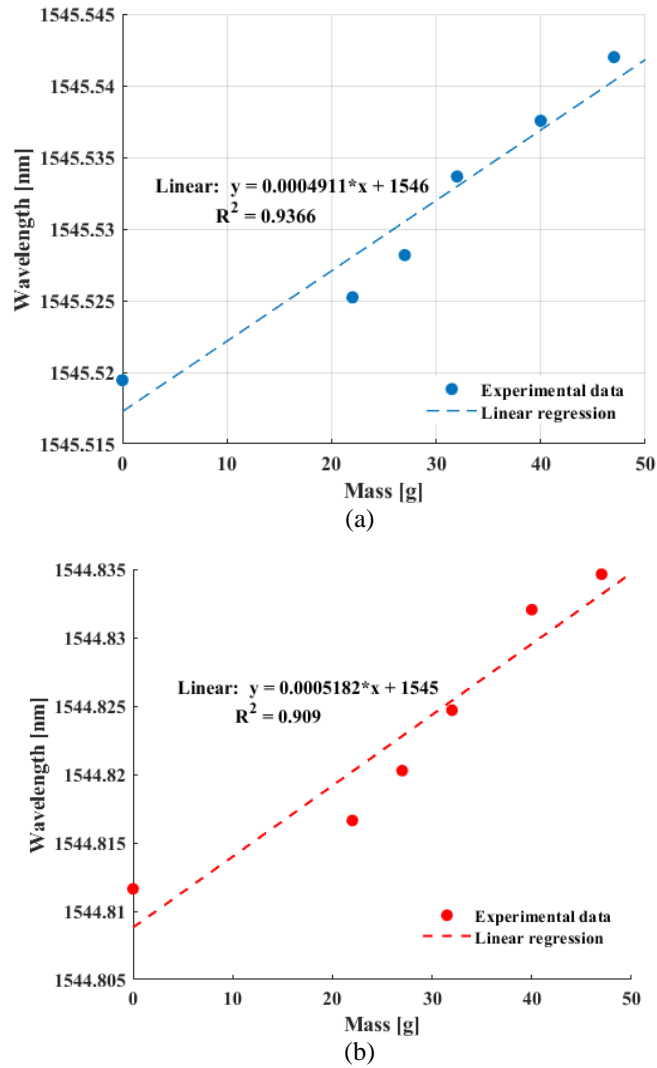


Figure 7. Mass deposition sensor for (a) FBG 1 and (b) FBG 2.

According to Figure 7, the reflected Bragg wavelength shifted linearly with the mass deposited in both cases. Linear regression was used to fit the data for FBG 1, resulting in a sensitivity of  $0.0004911 \text{ g/nm}$ . In the case of FBG 2, linear regression was applied, leading to a sensitivity of  $0.0005182 \text{ g/nm}$ .

As there are two variables (mass and temperature), two sets of equations (sensitivities of sensor 1 and 2) are needed to reach a determined system, that is, a system with a unique solution. Thus, the matrix Equation 5 can be formulated.

$$\begin{bmatrix} Dm \\ DT \end{bmatrix} = \begin{bmatrix} K_{m,\lambda_1} & K_{T,\lambda_1} \\ K_{m,\lambda_2} & K_{T,\lambda_2} \end{bmatrix}^{-1} \begin{bmatrix} D\lambda_1 \\ D\lambda_2 \end{bmatrix} \quad (5)$$

Where K is the sensitivity of FBGs 1 ( $\lambda_1$ ) and 2 ( $\lambda_2$ ) in relation to mass (m) and temperature (T).

When using one of the optical fibers to compensate for the effect of temperature variation, the variation in the Bragg wavelength, that is, the wavelength reflected by the Bragg gratings, becomes a function only of the mechanical deformation imposed on the optical fiber. In the experiments carried out, the dominant effect responsible for the

mechanical deformation is the deposition of the mass of the precipitate on the sensitive region. The results obtained are in accordance with Figure 8.

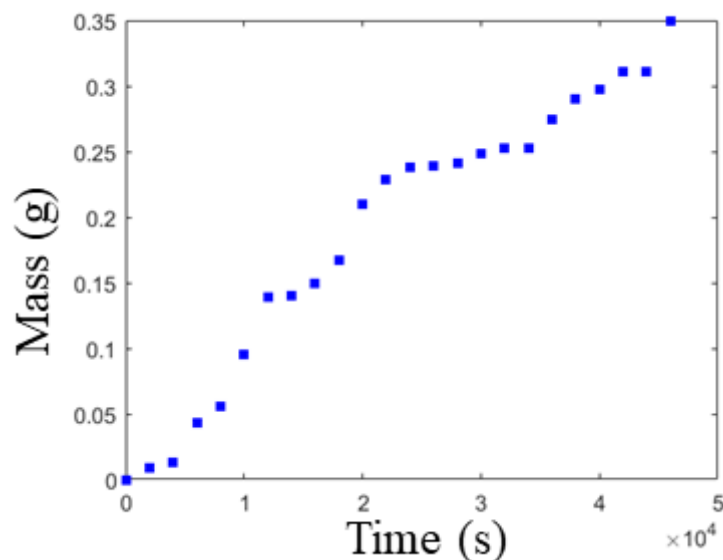


Figure 8. Mass deposited on the optical fiber over the experiment time.

From the sensor characterization shown in Figure 7, the mass deposition of the precipitate was monitored during the test time, as shown in Figure 8. As shown in Figure 2, the mass deposition after performing the experimental procedure, that is, after the chemical reaction of  $\text{CaCO}_3$  formation, was approximately 3 grams. Considering a uniform distribution of the mass deposited on the sensor plate, approximately 0.3 grams of precipitate is estimated over the sensitive region of the optical fiber. At the end of the experiment, the value estimated by the sensor was 0.35 grams of precipitate over the sensitive region. Thus, the type of sensor used for monitoring fouling is promising for its ability to monitor mass deposition, as performed in the experimental procedures performed.

## 6. FINAL REMARKS

The tests carried out in this article were intended to prove the concept of mass measurement by FBG, with estimates using only physical models.

With one of the optical fibers being used to compensate for the effect of temperature variation, the variation in the Bragg wavelength is a function only of the mechanical deformation imposed on the optical fiber. Thus, the deposition of the mass of the precipitate on the sensitive region is responsible for the mechanical deformation. This process is promising for predicting the mass of calcium carbonate deposited in the study system.

The future step of this work will be the implementation of sensors in the test system and application of artificial intelligence algorithms to improve the performance of the sensors.

## 7. ACKNOWLEDGEMENTS

The authors thank Petrobras for the financial support provided and the Federal University of Espírito Santo for the infrastructure to carry out the experimental tests

## 8. REFERENCES

- A. G. Leal-Junior, A. Theodosiou, C. Marques, M. J. Pontes, K. Kalli and A. Frizera, "Compensation Method for Temperature Cross-Sensitivity in Transverse Force Applications With FBG Sensors in POFs," in *Journal of Lightwave Technology*, vol. 36, no. 17, pp. 3660-3665, 1 Sept.1, 2018.
- Al Nasser, W. N.; Shaikh, A.; Morriss, C.; Hounslow, M. J.; Salman, A. D. Determining kinetics of calcium carbonate precipitation by inline technique. *Chemical Engineering Science*, 63, p. 1381-1389. Elsevier, 2008
- Christian Broadway, Rui Min, Arnaldo Gomes Leal-Junior, Carlos Marques, and Christophe Caucheteur, "Toward Commercial Polymer Fiber Bragg Grating Sensors: Review and Applications," *J. Lightwave Technol.* 37, 2605-2615 (2019)

- Cowan, J. C.; Weintritt, D. J. Water-formed scale deposits. Houston, TX: Gulf Publishing Company, 1976.
- Crabtree, M.; Eslinger, D.; Fletcher, P.; Miller, M.; Johnson, A.; King, G. Fighting scale—removal and prevention. *Oilfield Review*, p. 30-45, Autumn, 1999.
- Davies, M.; Scott, P. J. B. Oilfield water technology. Houston, TX: NACE International, 2006.
- Frenier, W. W.; Ziauddin, M. Formation, removal and inhibition of inorganic scale in the oilfield environment. Richardson, TX:185 Society of Petroleum Engineers (SPE Books), 2008.
- Golnabi, H. Mass measurement using an intensity-modulated optical fiber sensor. *Optics and Lasers in Engineering*. 38. 537-548, 2002.
- Hamid, S., De Jesús, O., Jacinto, C., Izetti, R., Pinto, H., Droguett, E., ... & Batocchio, M. A. A practical method of predicting calcium carbonate scale formation in well completions. *Spe Production & Operations*, 31(01), 1-11, 2016.
- K. O. Hill and G. Meltz, "Fiber Bragg grating technology fundamentals and overview," in *Journal of Lightwave Technology*, vol. 15, no. 8, pp. 1263-1276, 1997.
- Martins, A. L., Santos, H. F, Castro, B. B., Gonçalves, A. S., Maffra, D. A., and J. B. Loureiro. "Large Scale Laboratory Tests for Calcium Carbonate Scaling in Sliding Sleeve Valves." Paper presented at the SPE International Oilfield Scale Conference and Exhibition, Virtual, June 2020.
- Moghadas, J.; Jamialahmadi, M.; Müller-Steinhagen, H.; Sharif, A.; Ghalambor, A.; Izadpanah, M. R.; Motaie, E. Scale formation in Iranian oil reservoir and production equipment during water injection. *Society of Petroleum Engineers*, SPE 80406, 5th International Oilfield Scale Symposium and Exhibition, Aberdeen, United Kingdom, 29–30 January, 2003.
- Muhammad Shahzad Kamal, Ibelwaleed Hussein, Mohamed Mahmoud, Abdullah S. Sultan, Mohammed A.S. Saad, Oilfield scale formation and chemical removal: A review, *Journal of Petroleum Science and Engineering*, Volume 171, 2018, Pages 127-139, ISSN 0920-4105
- Ramstad, K., Tydal, T., Askvik, K. M., & Fotland, P. Predicting carbonate scale in oil producers from high-temperature reservoirs. *SPE Journal*, 10(04), 363-373, 2005.
- Stiff, H. A., Davis, L.E. A method for predicting the tendency of oil field waters to deposit calcium sulfate. *J. Pet. Technol.* 4 (2), 25–28, 1952.
- W. J. Bock and A. W. Domanski, "High hydrostatic pressure effects in highly birefringent optical fibers," in *Journal of Lightwave Technology*, vol. 7, no. 8, pp. 1279-1283, 1989.
- Yap, J., Fuller, M. J., Schafer, L., & Kelkar, S. K. Removing Iron Sulfide Scale: A Novel Approach. *Society of Petroleum Engineers*. 2010
- York, J. L. and Schorle, B. J. Scale Formation and Prevention in Principles of Desalination, Chapter 10. pp. 497-514, 1966
- Zhang, Y., Shaw, H., Farquhar, R., et al. The kinetics of carbonate scaling-application for the prediction of downhole carbonate scaling. *J. Pet. Sci. Eng.* 29, 85–95. 2001.

## 9. RESPONSIBILITY NOTICE

The authors are the only responsible for the printed material included in this paper.